J. ISSS Vol. 3 No. 1, pp. 8-17, March 2014.
REGULAR PAPER

A Note on Modelling Directionality in Piezoresistivity

Sreenath Balakrishnan, Kaustubh Deshpande, and G.K. Ananthasuresh
Computational Nanoengineering (CoNe) Group and Mechanical Engineering
Indian Institute of Science, Bangalore 560012
Corresponding Author: bsreenat@mecheng.iisc.ernet.in

Keywords:
Piezoresistivity,
coordinate transformation,
fourth order tensor,
hybrid finite elements

Abstract

When computing the change in the electrical resistivity of a piezoresistive cubic material embedded in a deforming structure, the piezoresistive and the stress tensors should be in the same coordinate system. While the stress tensor is usually calculated in a coordinate system aligned with the principal axes of a regular structure, the specified piezoresistive coefficients may not be in that coordinate system. For instance, piezoresistive coefficients are usually given in an orthogonal Cartesian coordinate system aligned with the <100> crystallographic directions but designers sometimes deliberately orient a crystallographic direction other than <100> along the principal directions of the structure to increase the gauge factor. In such structures, it is advantageous to calculate the piezoresistivity tensor in the coordinate system along which the stress tensors are known rather than the other way around. This is because the transformation of stress will have to be done at every point in the structure but the piezoresistivity tensor needs to be transformed only once. Here, by using tensor transformation relations, we show how to calculate the piezoresistive tensor along any arbitrary Cartesian coordinate system from the piezoresistive coefficients for the <100> coordinate system. Some of the software packages that simulate the piezoresistive effect do not have interfaces for the calculation of the entire piezoresistive tensor for arbitrary directions. This warrants additional work for the user because not considering the complete piezoresisitive tensor can lead to large errors. This is illustrated with an example where the error is as high as 33%. Additionally, for elastic analysis, we used a hybrid finite element formulation that estimates stresses more accurately than the usual displacement-based formulation. Therefore, as shown in an example where the change in resistance can be calculated analytically, the percentage error of our piezoresistive program is an order of magnitude lower relative to the displacement-based finite element method.

1. Introduction

Piezoresistive effect is exhibited by some electrical conductors or semiconductors in which electrical resistivity changes due to mechanical stress (Sze 1994). Sensors based on the piezoresistive effect are widely used in the industry today to build a variety of micro-electro-mechanical-

Available online at www.isssonline.in/journal/03paper02.pdf Paper submitted on December 1, 2013. Accepted on March 10, 2014.

systems (MEMS) devices. They include sensors for pressure (Buchhold *et al*. 2000), acceleration (Plaza *et al*. 2000), tilt (Bychkovsky *et al*. 2010), force (Bychkovsky *et al*. 2010), etc. These sensors need a piezoresistive material embedded in an elastically deforming structure. The mechanical structure acted upon by external forces develops stress, which in turn produces a change in the electrical resistance of the piezoresistor. The change in resistance is measured using a variety of techniques (e.g., Wheatstone's bridge circuit) that give a measure of the stress in the structure that can be further used to estimate the measurand that caused the stress.

Analytical techniques (Bao *et al*. 1989; Song *et al*. 1991; Gridchin *et al*. 1997; Kon *et al*. 2007) are widely used for the analysis of piezoresistors of standard shapes. The resistance change of the piezoresistive material is related to its strain by a quantity known as the *gauge factor*. The gauge factor *GF* is defined as,

$$GF = \frac{\Delta R/R}{\varepsilon} \tag{1}$$

where $\vec{j}$ is the change in resistance caused by strain, R the original resistance, and ε the strain. But the use of such analytical techniques restricts the shapes of the resistors that satisfy the underlying assumptions. Analysis of irregular and non-standard shapes is not possible with these techniques.

Numerical methods have been developed for analyzing the piezoresistive effect mainly by employing the finite element method (Buchhold *et al*. 2000; Plaza *et al*. 2000; Hsieh *et al*. 2001; Plaza *et al*. 2002). Numerical estimation of the piezoresistive effect is usually done by solving the electric conduction equation

$$\nabla \cdot \vec{J} = 0 \tag{2}$$

where $\vec{j}$ is the current density vector. The current density can be related to the electric field by using Ohm's law

$$\vec{J} = \tilde{\gamma}\vec{E} \tag{3}$$

where $\tilde{\gamma}$ is the conductivity matrix and $\vec{E}$ the electric field. The conductivity and electric field are related to the resistivity and potential according to the relations

$$\begin{aligned} \tilde{\gamma} &= \tilde{\rho}^{-1} \\ \vec{E} &= \nabla\Phi \end{aligned} \tag{4}$$

The resistivity is modelled up to the first order in terms of stress.

$$\tilde{\rho} = \rho_0 \left\{ \mathrm{I} + \tilde{\pi} : \tilde{\sigma} \right\} \tag{5}$$

where ρ_0 is the resistivity in the unstressed state, $\tilde{\pi}$ the fourth order piezoresistivity tensor and $\tilde{\sigma}$ the second order stress tensor and ':' is the operation of the fourth order tensor on the second order tensor to give the change in resistivity as a second order tensor. This requires the piezoresistive and stress tensors to be known in the same coordinate system, and this may not be readily ascertained.

The values of the piezoresistive coefficients that comprise the piezoresistive tensor are usually given in a coordinate system along the <100> crystallographic directions. It may not always be convenient to calculate the stress tensor in that coordinate system. For example, if a piezoresistor is embedded in the cantilever, the piezoresistive tensor is given along the local coordinate system aligned with crystallographic directions, while it is convenient to calculate the stress tensor in the cantilever's coordinate system. The transformation of the stress to the crystallographic coordinate system is cumbersome, as the transformation will have to be performed at every point in the domain where the change in resistivity needs to be calculated. On the other hand, the piezoresistivity tensor is a property of the material. Thus, once transformed from the crystallographic direction to the cantilever's coordinate system, it will remain the same at every point in the domain.

In this paper, we show the transformation of the fourth order piezoresistive tensor from one Cartesian coordinate system to another and indicate that the transformed tensor can have more than the three independent coefficients that a cubic material has along a coordinate system aligned with the <100> crystal axes. We also show that approximating the transformed piezoresistive tensor to one with only three independent coefficients can sometimes lead to considerable errors in the calculated piezoresistive effect. This is significant because some of the software packages that

simulate the piezoresistive effect (for example, see CoventorWare; www.coventor.com) do not have convenient interfaces for the calculation of the complete piezoresistivity tensor when the crystal lattice is arbitrarily oriented with respect to the principal directions of the microsystem.

Based on the foregoing, in this note, we discuss the transformation of the piezoresistive tensor for use in coupled finite element calculations. This is done in Section 2. We present the details of modelling in Section 3 where we show a possible error when the user-interface of software compels the user to ignore certain terms in the transformed piezoresistive tensor. In Section 4, we describe the hybrid finite element method that is more accurate in estimating stresses than the traditionally used displacement-based finite element method. Section 5 contains a discussion and concluding remarks.

2. Coordinate Transformation of the Fourth Order Piezoresistive Tensor

The piezoresistivity tensor (see Eq.(5)) has both minor and major symmetries and hence requires only 36 independent components (instead of 81 in the case of a general fourth order tensor) and can be written as a 6 × 6 matrix (Senturia 2001). For cubic materials, the piezoresistivity tensor measured in a coordinate system aligned along the <100> lattice directions has additional symmetries due to which, the piezoresistivity tensor contains only three independent coefficients (Senturia 2001) and can be written as

$$\tilde{\pi}_{\langle 100\rangle} = \begin{bmatrix} \pi_{11} & \pi_{12} & \pi_{12} & 0 & 0 & 0 \\ \pi_{12} & \pi_{11} & \pi_{12} & 0 & 0 & 0 \\ \pi_{12} & \pi_{12} & \pi_{11} & 0 & 0 & 0 \\ 0 & 0 & 0 & \pi_{44} & 0 & 0 \\ 0 & 0 & 0 & 0 & \pi_{44} & 0 \\ 0 & 0 & 0 & 0 & 0 & \pi_{44} \end{bmatrix} \tag{6}$$

where the compression of the indices has been done according to the convention, 11 $\rightarrow$ 1, 22$\rightarrow$2, 33$\rightarrow$3,12$\rightarrow$4, 23$\rightarrow$5, 31$\rightarrow$6. This means that the coefficient at the (4, 5) position in the matrix notation of the piezoresistive tensor is actually in the (1,2,2,3) position of the fourth order tensor.

The transformation of second order tensors between two Cartesian coordinate systems is given as (Jog 2007)

$$\tilde{T}' = [R]\tilde{T}[R]^{-1} \tag{7}$$

where [R] is the rotation matrix between the two coordinate systems given by

$$[R] = \begin{bmatrix} l_1 & l_2 & l_3 \\ m_1 & m_2 & m_3 \\ n_1 & n_2 & n_3 \end{bmatrix} \tag{8}$$

and the directions of the coordinate axes of the rotated coordinate systems in the original coordinate system are

$$x' = \begin{bmatrix} l_1 \\ m_1 \\ n_1 \end{bmatrix}, y' = \begin{bmatrix} l_2 \\ m_2 \\ n_2 \end{bmatrix}, z' = \begin{bmatrix} l_3 \\ m_3 \\ n_3 \end{bmatrix} \tag{9}$$

In the case of symmetric second order tensors, they can be represented as a 6-element column vector using the same convention for the compression of indices used in Eq.

$$\tilde{T}^T = \{T_1 \quad T_2 \quad T_3 \quad T_4 \quad T_5 \quad T_6\} \tag{10}$$

Using the vector representation of the symmetric second order tensor shown in the preceding equation, the coordinate transformation can be effected using a single 6 × 6 rotation matrix multiplication

$$\tilde{T}' = [R]_{6\times 6}\,\tilde{T} \tag{11}$$

where $[R]_{6x6}$ is given by

$$\begin{bmatrix} l_1^2 & m_1^2 & n_1^2 & 2l_1m_1 & 2m_1n_1 & 2n_1l_1 \\ l_2^2 & m_2^2 & n_2^2 & 2l_2m_2 & 2m_2n_2 & 2n_2l_2 \\ l_3^2 & m_3^2 & n_3^2 & 2l_3m_3 & 2m_3n_3 & 2n_3l_3 \\ l_1l_2 & m_1m_2 & n_1n_2 & l_1m_2+l_2m_1 & m_1n_2+m_2n_1 & n_1l_2+n_2l_1 \\ l_2l_3 & m_2m_3 & n_2n_3 & l_2m_3+l_3m_2 & m_2n_3+m_3n_2 & n_2l_3+n_3l_2 \\ l_3l_1 & m_3m_1 & n_3n_1 & l_3m_1+l_1m_3 & m_3n_1+m_1n_3 & n_1l_3+n_1l_3 \end{bmatrix} \tag{12}$$

Analogous to the case of second order tensors, the coordinate transformation of fourth order tensors is given by (Jog 2007)

$$\tilde{\pi}' = [R]_{6\times 6}\,\tilde{\pi}\,[R]^{-1}_{6\times 6} \tag{13}$$

For the case where the transformed coordinate system differs from the original coordinate system only through a rotation about the z-axis the transformed piezoresistive tensor expression reduces to a 6x6 matrix:

$$\tilde{\pi}' = \begin{bmatrix} \frac{3\pi_{11}+\pi_{12}+\pi_{44}+(\pi_{11}-\pi_{12}-\pi_{44})\cos(4\theta)}{4} \\ \frac{\pi_{11}+3\pi_{12}-\pi_{44}-(\pi_{11}-\pi_{12}-\pi_{44})\cos(4\theta)}{4} \\ \pi_{12} \\ \frac{(-\pi_{11}+\pi_{12}+\pi_{44})\sin(4\theta)}{4} \\ 0 \\ 0 \end{bmatrix}$$

$$\begin{matrix} \frac{\pi_{11}+3\pi_{12}-\pi_{44}-(\pi_{11}-\pi_{12}-\pi_{44})\cos(4\theta)}{4} \\ \frac{3\pi_{11}+\pi_{12}+\pi_{44}+(\pi_{11}-\pi_{12}-\pi_{44})\cos(4\theta)}{4} \\ \pi_{12} \\ -\frac{(-\pi_{11}+\pi_{12}+\pi_{44})\sin(4\theta)}{4} \\ 0 \\ 0 \end{matrix} \qquad (14)$$

$$\begin{bmatrix} \pi_{12} & \frac{(-\pi_{11}+\pi_{12}+\pi_{44})\sin(4\theta)}{2} & 0 & 0 \\ \pi_{12} & -\frac{(-\pi_{11}+\pi_{12}+\pi_{44})\sin(4\theta)}{2} & 0 & 0 \\ \pi_{11} & 0 & 0 & 0 \\ 0 & (\pi_{11}-\pi_{12}-\pi_{44})\sin^2(2\theta)+\pi_{44} & 0 & 0 \\ 0 & 0 & \pi_{44} & 0 \\ 0 & 0 & 0 & \pi_{44} \end{bmatrix}$$

where θ is the angle of rotation about the z-axis of the transformed coordinate system with respect to the original coordinate system.

3. Modelling Piezoresistivity using the complete Piezoresistive Tensor

Piezoresistive modelling software such as CoventorWare does not have convenient interfaces for specifying the piezoresistive tensor when the <100> crystallographic axes of the piezoresistive material are oriented in an arbitrary direction to the coordinate directions in which the stresses are known. For instance, CoventorWare will calculate the total piezoresistive tensor from the tensor specification along the <100> directions for the following crystallographic orientations:

1) x-axis along <110> and axis along <100>

2) -axis and -axis along <110>

3) -axis along <110 and axis along <111>

For other orientations of the crystallographic axes, one needs to manually compute the piezoresistive tensor (using Eq. (13)) and enter the complete 6 × 6 piezoresistive tensor into a text file containing properties. We show, by using relevant microsystems designs, that specifying the complete piezoresistive tensor is necessary and that any approximation of the same using a three independent coefficient tensor of the same form as in Eq(6). can lead to substantial errors.

The error in some of the piezoresisitve coefficients π'_{11}, π'_{12} and π'_{44} when only the three piezoresistive coeffiecents (as given in Eq. (14)) are used to construct the complete piezoresistive tensor was calculated using Eq. (6). This error for different orientations of the crystal axes is given in Figure 1. The values of the piezoresistive coefficient for p-type silicon are: $\pi_{11} = 6.6\times10^{-11}\,\text{Pa}^{-1}$ $\pi_{12} = -1.1\times10^{-11}\,\text{Pa}^{-1}$, and $\pi_{44}=1.381\times10^{-9}\,\text{Pa}^{-1}$ (Smith 1954; Senturia 2001).

A micromirror, where such inaccuracies in the estimation of the piezoresistive tensor leads to significant errors in the simulation results, is shown in Figure 2. The micromirror was actuated by applying an out-of-plane distributed load on the faces AB and CD in opposite directions such that the supporting bars twist. The piezoresistive effect in the embedded piezoresistor was quantified using a Wheatstone quarter bridge circuit as shown in Figure 3.

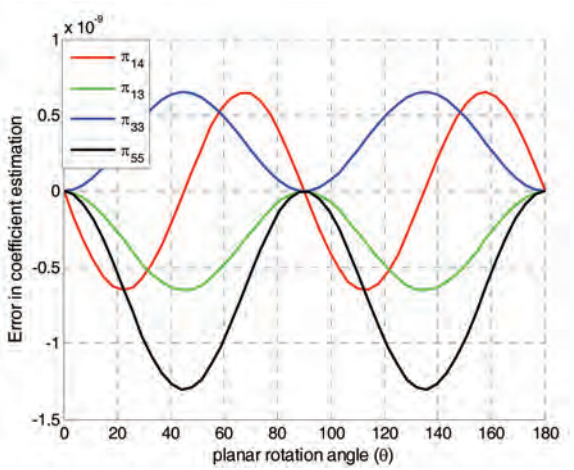

Figure 1: Variation of error in the estimated piezoresistive coefficient with crystal axes orientation

Both simulations, when using the approximate piezoresistive tensor having only three independent coefficients (Eq.(6)) and when using the complete rotated piezoresistive tensor (Eq. (14)), were done in COMSOL (www.comsol.com). Even though COMSOL does not have a piezoresistivity module, there are convenient interfaces which allow one to

use COMSOL for piezoresistive analyses. In the *'Electric Currents'* module of COMSOL, the electric conductivity can be specified as a function of any number of known variables. Symbolic math packages were used to compute the exact dependence of electrical conductivity on stress and the piezoresistive coefficients. The second order resistivity tensor was expressed in terms of stress and piezoresistive coefficients (Eq.(5)) and then they were inverted to get the expression for electrical conductivity (Eq.(4)) in terms of the piezoresistive coefficients and stresses. The resulting terms were entered in COMSOL. The structural deformation and stresses in the microsystem was calculated using the *'Solid Mechanics'* module and then the *'Electric Currents'* module was run in which electrical conductivity is expressed as a function of the stresses and the piezoresistive coefficients. A voltage of 5 V and 0 V was applied on opposite ends of the piezoresistor and the total current was estimated by integrating the current density on the end surface.

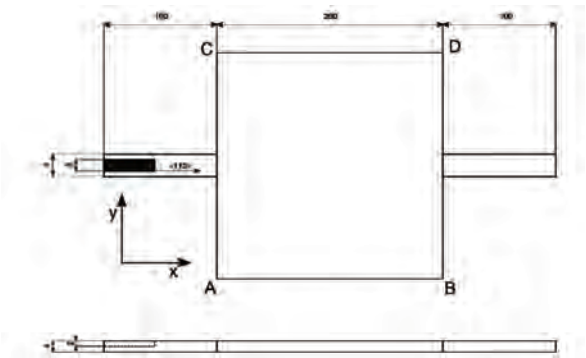

Figure 2: Micromirror supported by two beams of square cross-section fixed at the ends. The material is assumed to be linear elastic E=169GPa and í=0.22 (silicon). P-type silicon $\rho_0 = 7.8\times10^{-2}\,\Omega\text{m}$, $\pi_{11} = 6.6\times10^{-11}\,\text{Pa}^{-1}$ $\pi_{12} = -1.1\times10^{-11}\,\text{Pa}^{-1}$ and $\pi_{44}=1.381\times10^{-9}\,\text{Pa}^{-1}$ have been used (Smith 1954; Senturia 2001). All dimensions are in μm.

$$I = \int_s \vec{J}.\vec{ds} \tag{15}$$

The total resistance of the piezoresistor was then estimated using Ohm's law

$$R_{PZR} = \frac{V}{I} \tag{16}$$

The voltage output of the Wheatstone's quarter bridge circuit (Figure 3) was calculated as

$$V_{out} = \frac{R_{PZR}R_0 - R_0^2}{\left(R_{PZR}+R_0\right)\left(2R_0\right)}V_{in} \tag{17}$$

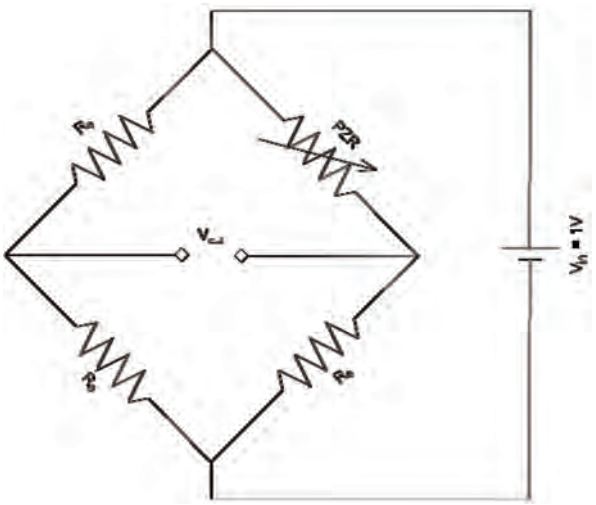

Figure 3: Wheatstone quarter bridge configuration used to quantify the piezoresistive effect. The constant resistance R_0 is equal to the resistance of the piezoresistor when there is no stress.

The voltage output (V_{out}) of the Wheatstone quarter bridge circuit for different actuation forces on the micromirror is given in Figure 4A. The percentage error in the output voltage when using only three independent coefficient piezoresisitive tensor (see Eq.(6)) is shown in Figure 4B. The percentage error is calculated as

$$\%\text{error} = \frac{\left(V_{out}\right)_{3\text{ ind. }\pi} - \left(V_{out}\right)_{\text{comp. }\pi}}{\left(V_{out}\right)_{\text{comp. }\pi}} \times 100 \tag{18}$$

It can be observed that there is a substantial difference in the simulated results when using the complete piezoresistive tensor leading to up to a 33% error in the voltage output as compared to using only three-independent-term piezoresistive tensor.

Next, we discuss the hybrid finite element formulation that gives stress with enhanced accuracy as compared to the displacement-based finite element method. This leads to a further improvement in calculating the coupled effects of pizeoresistivity caused by the stress.

4. Hybrid Element Formulation

The hybrid finite element formulation is a two-field formulation in which the displacements and

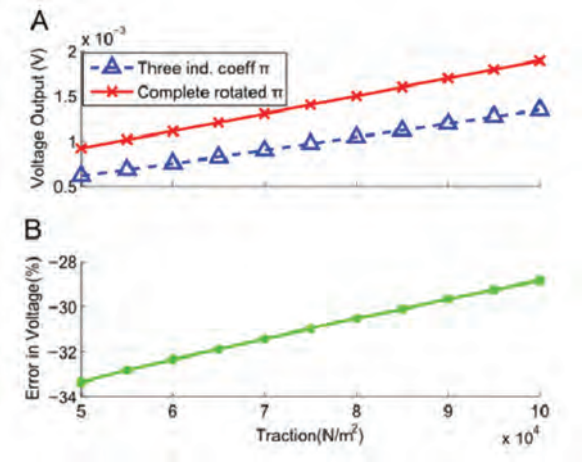

Figure 4: Comparison of piezoresistive simulation results when using only three independent coefficients for the piezoresistive tensor and when using the complete rotated piezoresistive tensor. (A) Voltage output V_{out} of the Wheatstone quarter bridge circuit for various actuating forces on the micromirror (B) Error in the output voltage V_{out} as a percentage of the output voltage.

stresses are interpolated independently. The weak form of the variational equations used are (Jog 2005; Jog *et al*. 2006; Jog 2010)

$$\int_{\Omega} \boldsymbol{\tau} : \boldsymbol{\varepsilon}(\delta\mathbf{u})\, d\Omega - \int_{\partial\Omega_t} \delta\mathbf{u} \cdot \mathbf{f}_t\, d(\partial\Omega) - \int_{\Omega} \delta\mathbf{u} \cdot \mathbf{f}_b\, d\Omega = 0 \quad \forall \delta\mathbf{u} \qquad (19)$$

$$\int_{\Omega} \delta\boldsymbol{\tau} : \left\{ \boldsymbol{\varepsilon}(\mathbf{u}) - \mathbf{D}^{-1} : \boldsymbol{\tau} \right\} d\Omega = 0 \quad \forall \delta\boldsymbol{\tau} \qquad (20)$$

where Ω is the domain occupied by the solid, dΩ is the boundary, f_b and are respectively the body and surface forces, **u** is the displacement field, τ is the stress field, ε is the strain field, **D** is the constitutive material relationship relating the stress with the strain and δu and δτ are arbitrary variations in the displacement and stress fields respectively. The interpolation functions for the stresses are constructed so as to avoid the 'locking' behaviour exhibited by normal displacement-based finite elements (Jog *et al*. 2006; Jog 2010).

The hybrid element formulation is unaffected by skewed elements and are hence ideal for analysing geometries with the high aspect ratios typically found in microsystems. Also such a formulation gives improved accuracy for the estimated stress field as compared to displacement based finite element methods for the same mesh (Sundaram *et al*. 2012).

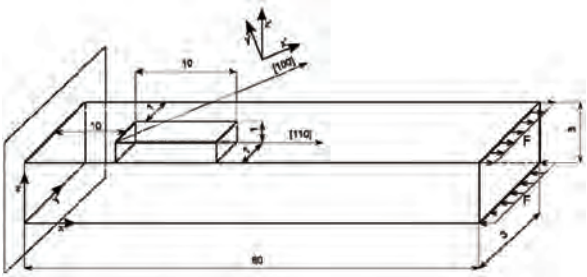

Figure 5: A cantilever fixed at one end and loaded at the other by a couple. The material is assumed to be linear elastic E=170GPa and μ=0.28. All dimensions are in μm

Table 1: Meshes used for the piezoresistive simulations

Meshes	Cantilever	Piezoresistor
Mesh 1	60x3x3 = 540 elements	10x1x1 = 10 elements
Mesh 2	60x6x6 = 2160 elements	10x2x2 = 40 elements

The higher accuracy in the estimated stress will lead to improved estimation of the piezoresistive effect. To demonstrate this, a comparison was made between the simulated piezoresistive effects for a displacement based (CoventorWare) and hybrid elements based finite element method (i.e., our implementation) with the analytical solution.

The piezoresistive simulation considered was that of a cuboidal piezoresistor embedded in a cantilever beam (see Figure 5). The simplistic nature

Table 2: Patch currents and comparison between CoventorWare and hybrid simulations

Mesh	Patch Current		% error in Patch Current	
	CoventorWare	Hybrid	CoventorWare	Hybrid
Mesh 1	6.3721μA	6.3698 μA	0.0392	0.0031
Mesh 2	6.3717 μA	6.3697 μA	0.0330	0.0016

of the geometries involved is warranted for it to be possible to calculate an analytical solution. To enhance the piezoresistor sensitivity, the [110] crystallographic direction was aligned with the x-axis since the π_{11} coefficient is maximum along the [110] direction (Eq. (14)).P-type silicon ρ_0=7.8x10-2Ωm, π_{11}=6.6x10^{-11}Pa^{-1}, π_{11}=-1.1x10^{-11}Pa^{-1} and π_{44}=1.381x10^{-9}Pa^{-1} have been used (Smith 1954; Senturia 2001)**.**

For the slender cantilever beam structure analyzed, it can be assumed that the stress field consists of only normal stress along the x direction, namely σ_{xx}, in Euler-Bernoulli beam theory. The other stresses are at least two orders of magnitude smaller. The cantilever was loaded with a moment (couple) at the free end and not a force so that there are no shear stresses of magnitude comparable to the normal bending stresses. The expression for the total resistance of the piezoresistive element can be obtained by integrating the resistances of the individual infinitesimal resistors.

The resistance of the infinitesimal slab *dR(z)* (see Figure 6) can be obtained by integrating the infinitesimal strips along the x-axis. It entails a straightforward integration as all the infinitesimal resistance strips forming *dR(z)* are connected in series.

$$dR(z) = \int_0^L \frac{\rho dx}{wdz} \tag{21}$$

where is the resistivity of the element, *dx* is the length of the element and *wdz* is the cross-sectional area. The resistivity can then be approximated as

$$\rho = \rho_0 \left(1 + \pi_{11}\sigma_{xx}\right) \tag{22}$$

since the voltage difference is applied only along the length of the resistor and all other stress values are at least two orders of magnitude smaller than the normal stresses. Substituting for σ_{xx} from the Euler-Bernoulli beam theory we get

$$\begin{aligned} dR(z) &= \int_0^L \frac{\rho_0}{wdz}\left(1 + \pi_{11}\frac{Mz}{I}\right)dx \\ &= \frac{\rho_0 L}{wdz}\left(1 + \pi_{11}\frac{Mz}{I}\right) \end{aligned} \tag{23}$$

since the integration is only along the x direction where *M* is the moment at the section, *z*

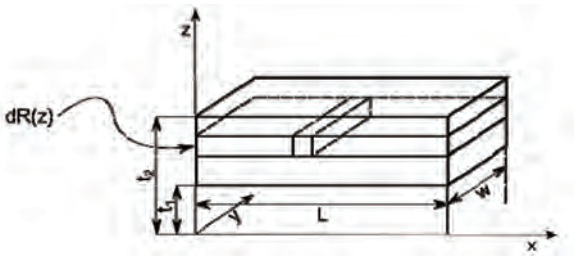

Figure 6: Finding the equivalent resistance along the x-axis of a cuboidal piezoresistor of dimensions L x w x t. The piezoresistor is decomposed into slabs dR(z) which are connected in parallel. Each of the slabs are in turn made up of strips connected in series.

is the distance of the resistor from the neutral axis and *I* is the moment of inertia of the cross-section.

The effective resistance can be obtained by finding the total resistance of such infinitesimal resistance slabs *dR(z)* that are connected in parallel.

$$\begin{aligned} \frac{1}{R} &= \int_{t_1}^{t_2} \frac{1}{dR(z)} \\ &= \int_{t_1}^{t_2} \frac{w}{\rho_0 L}\frac{dz}{\left(1 + \frac{\pi_{11}Mz}{I}\right)} \end{aligned} \tag{24}$$

$$R = \frac{\rho_0 L \pi_{11} M}{wI \log\left\{\frac{1 + \left(\pi_{11}Mt_2/I\right)}{1 + \left(\pi_{11}Mt_1/I\right)}\right\}} \tag{25}$$

This can be written in the standard form

$$R = \frac{\rho L}{w\left(t_2 - t_1\right)} \tag{26}$$

By defining the effective resistivity ρ as

$$\rho = \frac{\rho_0\left(t_2 - t_1\right)}{t_{eff} \log\left\{\frac{1 + \left(t_2/t_{eff}\right)}{1 + \left(t_1/t_{eff}\right)}\right\}} \tag{27}$$

where the effective thickness t_{ejj} is

$$t_{eff} = \frac{I}{\pi_{11}M} \tag{28}$$

For the geometry and material properties shown in Figure 6, the total resistance was calculated to be 7.8498x10^{5}Ω which gives the current for an applied voltage of 5 V to be equal to .

The piezoresistive effect for the geometry and material properties shown in Figure 6 was simulated

in both CoventorWare and our implementation that uses hybrid elements for analysing elastic deformation. Two meshes (see Table 1) consisting of rectangular brick elements of different sizes were used for the convergence study. Further mesh sizes were not considered since our implementation had already converged sufficiently with the analytical result.

Table 2 shows that, for the problem considered, the hybrid implementation is at least an order of magnitude less prone to error as compared to the displacement-based finite element techniques even though for such simple geometries the error in the simulated piezoresistive effect itself is very small even for the displacement-based finite element method. But for complicated geometries of relevant microsystems, as has been shown previously (Sundaram *et al*. 2012), the finite element method based on hybrid elements can produce improved convergence for the structural analysis. Since accurate estimation of stresses leads to an improvement in the calculated piezoresistive effect, we believe that the use of hybrid elements in structural analysis is beneficial.

5. Discussion and Closure

The error in the simulated piezoresistive effect when not using the complete piezoresistive tensor depends on the nature of the stress field. The piezoresistive coefficients π'_{11},π'_{12},π'_{21}, and π'_{22} can be estimated accurately even when only the approximate piezoresistive tensor consisting of only three independent terms (see Eq.(6)) is used. Hence, while simulating microsystems having only tensile or compressive stress in the *yz* and *xz* planes (σ_{xx} and σ_{yy}), the error in the simulated piezoresistive effect when using only these coefficients will be very small. Some examples of such microsystems are slender beams used in micromechanical suspensions, membranes used in pressure sensors, etc.

Another factor contributing to the error in the simulated piezoresistive effect when approximating the piezoresistive tensor is the relative magnitude of the piezoresistive coefficients in the particular orientation of the crystal axes. If the error in the estimation of the piezoresistive coefficients is small when compared with the value of the accurately estimated piezoresistive coefficients (π'_{11},π'_{12} and π'_{44}), the overall inaccuracy in the estimation of the piezoresistive effect will be small. In the micromirror example shown in Figure 3, the piezoresistive coefficients with independent non-zero errors are, π'_{13},π'_{33} and π'_{55} and with respective errors equal to $-6.52\times10^{-10}Pa^{-1}$and $-1.304\times10^{-9}Pa^{-1}$(see Figure 1) while the values of the accurately estimated piezoresistive coefficients is $\pi'_{11}=7.18\times10^{-10}Pa^{-1}$, $\pi'_{12}=-6.63\times10^{-10}Pa^{-1}$ and $\pi'_{44}=7.7\times10^{-11}Pa^{-1}$. The error in estimation of the piezoresistive coefficients is comparable to the accurately estimated coefficients. Moreover there is a substantial amount of shear stresses in the microsystem, especially τ_{xz} which multiplies with the piezoresistive coefficient with the highest error in estimation π'_{66} , which results in large inaccuracies in the estimation of the piezoresistive effect. The errors in the estimation of π'_{55} and $\pi'_{66}$are equal.

As illustrated here, the coordinate transformation of the piezoresistive tensor improves the accuracy of a piezoresistive simulation. It is worth noting that it involves a simple calculation. The errors when approximating the piezoresistivity tensor with a three independent coefficient tensor may be small in the cases when the microsystem has larger normal stresses as compared to shear stresses. We have presented a case where there are high shear stresses leading to substantial error in the simulated piezoresistive effect. In our implementation of the piezoresistive analysis we have incorporated an interface for specifying the direction cosines of the <100> crystallographic directions (Eq. (9)) with respect to the coordinate system in which the stresses are known for facilitating the calculation of the complete piezoresistive tensor oriented in an arbitrary direction to the principal axes of the microsystem.

It may also be noted that many microsystems have thin and narrow structures, which should be discretized using very fine meshes in the displacement-based finite element method to avoid ill-conditioning that might arise in coarse meshes with elements of high aspect ratios. On the other hand, hybrid elements are not sensitive to the high aspect ratios of elements. Consequently, much fewer elements give accurate results in structural analysis done using hybrid elements (Sundaram

et al. 2012). Furthermore, a single element type can give accurate results for the analysis of all kinds of deformation problems. In the case of a piezoresistive analysis, as shown here, the increased accuracy of the stresses calculated by the hybrid finite element method will lead to an improved estimation of the piezoresistive effect.

Ackowledgement

This project was funded by the National Programme on Micro and Smart Systems (NPMASS). This support is gratefully acknowledged.

References

Bao, M. H., W. J. Qi and Y. Wang (1989). "Geometric design rules of four-terminal gauge for pressure sensors." Sensors and Actuators 18(2): 149-156.

Buchhold, R., R. Gollee, A. Nakladal and G. Gerlach (2000). "A novel approach to modeling the transfer functions of four-terminal-transducer pressure sensors within a single simulation tool." Sensors and Actuators A: Physical 80(1): 15-22.

Bychkovsky, V. and M. Lobur (2010). Piezoresistive cantilever for mechanical force sensors. Proceedings of the 2010 VI-th International Conference on Perspective Technologies and Methods in MEMS Design, IEEE.

Gridchin, A. and V. Gridchin (1997). "The four-terminal piezotransducer: theory and comparison with piezoresistive bridge." Sensors and Actuators A: Physical 58(3): 219-223.

Hsieh, M. C., Y. K. Fang, M. S. Ju, G. S. Chen, J. J. Ho, C. Yang, P. M. Wu, G. Wu and T. Y. F. Chen (2001). "A contact-type piezoresistive micro-shear stress sensor for above-knee prosthesis application." Journal of Microelectromechanical Systems 10(1): 121-127.

Jog, C. (2005). "A 27-node hybrid brick and a 21-node hybrid wedge element for structural analysis." Finite elements in analysis and design 41(11): 1209-1232.

Jog, C. (2007). Continuum Mechanics, Narosa Publishing House.

Jog, C. (2010). "Improved hybrid elements for structural analysis." Journal of Mechanics of Materials and Structures 5(3): 507-528.

Jog, C. and P. Kelkar (2006). "Non linear analysis of structures using high performance hybrid elements." International journal for numerical methods in engineering 68(4): 473-501.

Kon, S., K. Oldham and R. Horowitz (2007). Piezoresistive and piezoelectric MEMS strain sensors for vibration detection. Proc. of SPIE, Vol. 6529, 65292V.

Plaza, J. A., A. Collado, E. Cabruja and J. Esteve (2002). "Piezoresistive accelerometers for MCM package." Microelectromechanical Systems, Journal of 11(6): 794-801.

Plaza, J. A., J. Esteve and C. Cané (2000). "Twin-mass accelerometer optimization to reduce the package stresses." Sensors and Actuators A: Physical 80(3): 199-207.

Senturia, S. D. (2001). Microsystem design, Springer, Berlin.

Smith, C. S. (1954). "Piezoresistance effect in germanium and silicon." Physical review 94(1): 42.

Song, C., D. Kerns Jr, J. Davidson, W. Kang and S. Kerns (1991). Evaluation and design optimization of piezoresistive gauge factor of thick-film resistors. Proceedings of IEEE Southeastcon, IEEE, Vol. 2, pp. 1106-1109.

Sundaram, M., R. Ganesh, K. Pavan, B. Varun, C. Jog and G. Ananthasuresh (2012). Static Elastic Simulation of Micromechanical Structures using Hybrid Finite Elements. International Conference on Smart Materials Structures and Systems.

Sze, S. (1994). "Semiconductor sensors." John Wiley & Sons, New York.

Sreenath Balakrishnan received his BTech and MS in Mechanical Engineering from NIT Calicut in 2006 and Virginia Tech 2010 respectively. He is currently pursuing his PhD in Bioengineering at the Indian Institute of Science.

He has worked on design of submarines (INS Arihant) during a two year stint at Larsen and Toubro. There he has coded a new routine in CATIA

for the automation of pipe isometric drawings from 3D piping models. During his Masters he has worked on modeling the active ear deformations in horseshoe bats and demonstrated a novel target identification to target locating switch in the biosonar system through these deformations. Further he has modeled the kinematics of fingers in an algorithm for recognizing hand gestures when using a glove fitted with accelerometers during a six month internship at MindTree Foundation. Currently he is working on understanding the response of liver cells to mechanical stimuli. His research interests include mathematical modeling of biological systems, mechanobiology, biomechanics, tensegrity architecture and compliant mechanisms.

Kaustubh Deshpande is a product development engineer in the field of tape-library engineering. Kaustubh completed his graduate degree at Carnegie Mellon University and his undergraduate studies at Bits Pilani University. His research interests lie broadly in the field of Computational Engineering and particularly in the areas of meshing, multi-physics modeling, CAD and data analysis.

G.K. Ananthasuresh (B. Tech. IIT-Madras, 1989; MS, U. Toledo, 1991; PhD, Michigan, 1994) is a Professor of Mechanical Engineering at the Indian Institute of Science, Bangalore, India. His previous positions include post-doctoral associate at the Massachusetts Institute of Technology, Cambridge, USA; Associate Professor at the University of Pennsylvania, Philadelphia, USA; and visiting professorships in University of Cambridge, UK, and Katholike Univesiteit, Leuven, Belgium; and Indian Institute of Technology-Kanpur. His current research interests include compliant mechanisms, kinematics, multi-disciplinary design optimization, microsystems technology, micro and meso-scale fabrication, protein design, micromanipulation, and biomechanics of cells. He served on the editorial boards of ten journals and is a co-author of 75 journal papers and 135 conference papers as well as four edited books, one textbook, and 13 book-chapters. He has eight patents, three granted and five in process. He is a recipient of the NSF Career Award and SAE Ralph O Teeter Educational Award in the USA and the Swarnajayanthi Fellowship and Shanti Swarup Bhatnagar Prize in India as well as 10 best paper awards in international and national conferences and 6 prizes in design contests that his students and he participated.